9 November 2001

Chemical Physics Letters 348 (2001) 209–216

CHEMICAL PHYSICS LETTERS

www.elsevier.com/locate/cplett

Degenerate Four Wave Mixing on FeI atomic vapours during thermal decomposition of $Fe(CO)_5$: saturation and absorption effects

L. De Dominicis [a], M. Di Fino [a], R. Fantoni [a,*], S. Martelli [a], O. Bomatì Miguel [b], S. Veintemillas Verdagüer [b]

[a] *ENEA Applied Physics Division, Via E. Fermi 45, I-00044 Frascati (Rome), Italy*
[b] *Instituto de Ciencia de Materiales de Madrid, Cantoblanco, 28049 Madrid, Spain*

Received 2 August 2001; in final form 25 September 2001

Abstract

Thermal decomposition of $Fe(CO)_5$ vapours diluted in a buffer gas (Ar) was performed in a static optical cell heated up to 673 K. The nascent FeI formation in the gas phase was monitored by recording the Degenerate Four Wave Mixing (DFWM) spectrum of the a^5D_j–$y^5D^0_{j'}$ atomic transitions around 302 nm. Line-splitting phenomena, occurring upon strong saturation conditions at high laser power, were investigated on the DFWM lineshape. The role played by the absorption of exciting and signal beams in altering the relative lines intensities, predicted assuming an optically thin medium, is discussed and modelled in order to account for the experimental results.

1. Introduction

The atomic structure of neutral iron (FeI) has been exhaustively studied by several spectroscopic methods. Laser based techniques played a primary role in developing the accurate description of energy levels, lifetime and transition probabilities in FeI. The results of a large number of studies on iron are summarised in the National Institute of Standard and Technology (NIST) database [1], where as much as 2092 spectral line-positions are collected. Most of the spectroscopic measurements were performed on atomic Fe vapours by means of Laser Induced Fluorescence (LIF) [2], a technique currently used for the quantitative space resolved detection of FeI [3].

Degenerate Four Wave Mixing (DFWM) spectroscopy, a non-linear technique based on light scattering from laser induced gratings, is an effective alternative to LIF in order to detect traces of chemical species, since to a comparable sensitivity, DFWM adds a better space resolution. In DFWM experiments two pump laser beams with both the same wavelength λ_P and polarisation state, travel through the investigated medium forming with respect to each other an angle θ. If λ_P

* Corresponding author. Fax: +39-6-9400-5312.
E-mail address: fantoni@frascati.enea.it (R. Fantoni).

0009-2614/01/$ - see front matter
PII: S0009-2614(01)01140-X

matches with one of the allowed transitions of one or more chemical species in the medium, the generated pattern of optical fringes induces a sinusoidal modulation of the molecular internal energy and a modulation of the refraction complex index. This modulation originates, in turn, a grating able to diffract a fraction of a third degenerate probe beam (at wavelength λ_P) which is crossing the interaction region at the Bragg angle. In the last years DFWM on small molecules and radicals has been extensively studied, due to its potential for quantitative measurements of physical parameters (as for instance gas concentration and temperature) in chemically reacting media (e.g., flames and plasma) [4–6]. It has been found that DFWM signal is considerably less sensitive to collision quenching as compared to LIF, hence well suited for the detection of species at nearly atmospheric or higher pressure [7].

At the beginning in atomic vapours DFWM was mainly investigated because of the extremely high reflectivity (up to about 100%) observed from laser-induced gratings [8,9], a promising condition for the development of phase-conjugate mirrors based on atomic gases. Furthermore DFWM on atomic vapours was the object of special care due to laser beam saturation effects in the lineshape, which, first theoretically predicted, were experimentally observed in sodium vapours [10–12]. Highly saturated atomic DFWM lineshapes show, together with the usual broadening, a characteristic splitting when the laser is tuned at exact resonance with the probed transitions. Despite the partial knowledge on the physical mechanisms at the basis of the saturated lineshape splitting, this effect should be carefully accounted for any time DFWM is used for quantitative measurements in atomic vapours.

In the present contribution we report the results of DFWM detection of atomic iron produced by thermal dissociation of iron pentacarbonyl, $Fe(CO)_5$, a volatile oily complex which decomposes into $Fe + 5(CO)$ upon heating above 523 K. The FeI formation due to $Fe(CO)_5$ photo-fragmentation (photolysis) has been the subject of a large number of spectroscopic investigations [13–15], but only scant information is available for thermally induced dissociation [16]. In the present study the a^5D_j–$y^5D^0_j$ ($j = 2, 3, 4$) transitions of FeI, located around 302.06 nm, were investigated in an optical cell filled with a mixture of $Fe(CO)_5$ vapours diluted in Ar, where the thermal decomposition of the precursor was induced. In order to investigate the saturation effects the a^5D_2–$y^5D^0_2$ DFWM lineshape has been recorded at different values of pump laser energy. A theoretical simulation, based on the radiative re-normalisation method reported in [17], is proposed to explain the splitting mechanism.

The DFWM spectra collected far from saturation intensity showed, both at the high temperature (up to 673 K) and after cooling down the thermally decomposed mixture, line intensities characterised by strong deviations from the values expected for an optical thin medium at thermal equilibrium. A simplified analytical model is further presented to account for the wavelength dependent signal reduction, due to the absorption of incoming pump beams and of the generated signal beam.

2. Theoretical background

The DWFM signal intensity is proportional to the square of the third-order non-linear susceptibility and therefore depends on the square of the population difference N_{if} between the initial and final atomic level coupled by the resonant pump laser. Furthermore, in the limit of optical thin medium condition, it was found [5] that the integrated DFWM line intensity I_{if} is proportional to the square of the atomic line strength B_{if}

$$I_{if} \propto \left[B_{if}N_{if}\right]^2 I_P^2 I_{pr}, \tag{1}$$

where I_P and I_{pr} are, respectively, the pump and probe beam intensity. In thermal equilibrium at a temperature T, not sufficiently high for populating the upper level of the transition, N_{if} can be approximated by the numbers N_i of atoms in the lower state given by the Boltmann distribution

$$N_i \propto N g_i e^{-(E_i/kT)}, \tag{2}$$

where g_i and E_i are, respectively, the degeneracy and the energy of the lower atomic level, and N is

the atomic number density. From Eq. (2) results that the ratio between two DFWM spectral lines follows the thermal distribution of atoms in the excited levels probed.

Anyway, if the optically thin medium approximation $\alpha(\omega)L \sim 0$, with $\alpha(\omega)$ absorption coefficient and L length of the active medium, is not fulfilled, strong deviations in the DFWM line intensities ratio can be observed due to absorption effects on pumps, probe and signal beams. In particular, since the absorption coefficient is a nonlinear function of the number of atoms in the lower level, the signal reduction effects are more intense the stronger the DFWM lines (originated by the most populated levels at the temperature T) are. Furthermore, the nearly cubic dependence of the DFWM signal intensity on the exciting laser beam energy (when pumps and probe beams are assumed equally intense) contributes to enhance the absorption effects by altering line intensity ratio's. Although a complete theoretical treatment of pumps, probe depletion and signal absorption effects has been already proposed in the limit of non-saturating pump intensities [18], it requires awkward numerical solutions drastically limiting the range of application.

In the present DFWM experiment two pump beams with an intensity sufficient to saturate the one-photon probed transitions were used (see Section 3) together with a weaker probe beam, whose intensity is far below the saturation threshold. In order to model the experimental data we used a simplified model in which the absorption effect is comprehended, as a whole, in a single attenuation factor

$$I_{if} \propto \left[B_{if}N_i\right]^2\left(1-\alpha_{if}N_i\right)^{\beta}. \tag{3}$$

A further simplification was introduced by releasing the wavelength dependence of α_{if} and substituting this coefficient with an average value α, which assumes that only the absorption effect due to population differences between atomic levels is taken into account. The a-dimensional α, β parameters (the latter introduced as the exponent in the right factor of Eq. (3)) can be calculated from the measured lines intensities ratio at a given temperature and values obtained can be successively used to predict experimental results at different temperatures (i.e., to define a thermometric curve or to evaluate relative concentrations).

It should be mentioned that in the theoretical treatment neither the particle motion nor saturation effects on the DFWM signal intensity are considered. The hypothesis that particle motion can be neglected implies supposing that the atoms are frozen in their positions during the time duration of the exciting laser pulse and ascribing the observed line broadening entirely to collisional events. These assumptions are valid provided that the experimental condition $\Lambda \ll \lambda_T$ is fulfilled, where $\Lambda = \lambda_P/2\sin(\theta/2)$ is the fringe spacing and λ_T is the mean thermal displacement of an atom during the time duration of the laser pulse (split in contemporary pumps and probe beams).

Saturation effects in Forward DFWM (FDFWM) lineshape were formerly studied by using the radiative re-normalisation technique [17]. The relevant parameter S introduced in the model is defined as

$$S = \frac{\Omega^2}{\gamma_0\gamma_{ab}}, \tag{4}$$

where γ_0 and γ_{ab} are the population and collisional relaxation rate, respectively, while Ω is the Rabi frequency of the transition

$$\Omega = \frac{\mu_{ij}E_P}{\hbar} \tag{5}$$

with μ_{ij} the induced dipole moment of the probed transition and E_P the electric field strength of the pump beam. From Eqs. (4) and (5) the parameter S turns out to be non-dimensional. If the partial gas pressures and the temperature are kept fixed, S increases as pump laser power is raised. Any time the pump energy exceeds the saturation threshold level (corresponding to $S = 1$), the line broadening due to Rabi oscillations dominates the collisional width.

The theoretical FDWFM spectrum of the a^5D_2–$y^5D_2^0$ transition in FeI at different degree of saturation (i.e., different values of S) is reported in Fig. 1.

As predicted by the model, the fingerprint for the saturation of FDFWM lineshape is the appearance of a dip located at exact resonance of the

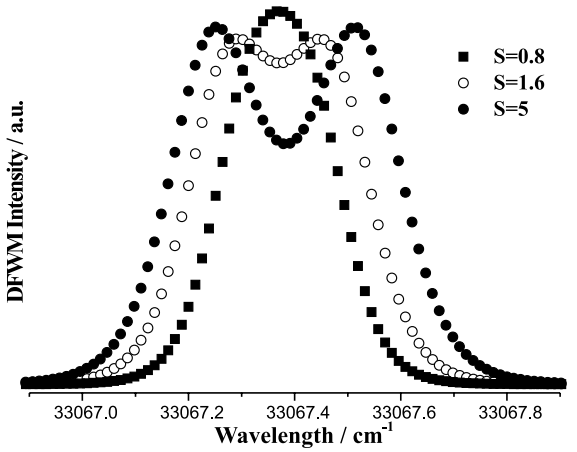

Fig. 1. FDWFM spectrum of the a^5D_2–$y^5D_2^0$ transition in FeI calculated for different values of the saturation parameter S. Details about the radiative re-normalisation model used are given in [17].

transition frequency and increasing with S. The model is capable of reproducing the line-splitting of saturated DFWM lines observed in the crossing pump beams geometry for the excitation of atoms, including iron, despite a comprehensive description of the physics underlying this phenomenon being still lacking.

In the absence of an adequate theory, the modelling of saturation effects must be based on an exhaustive experimental characterisation of each atomic species used as active medium, in order to avoid introducing errors in quantitative FDFWM measurements.

3. Experimental apparatus

The laser radiation for the excitation of the FeI a^5D_j–$y^5D_{j'}^0$ transitions was generated by frequency doubling in a BBOI crystal the output of a narrow-band dye laser operating with Rhodamin B. The dye laser was pumped by a doubled Nd:YAG laser (JK2000) providing up to 250 mJ per pulse at 532 nm with a repetition rate of 1 Hz. In this experimental scheme laser pulses in the spectral range between 300 and 310 nm were produced, with 15 ns of time duration and 600 μJ of energy. The bandwidth of the dye laser is specified to be 0.2 cm^{-1} by manufacturer. The FDFWM phase matching geometry [17], chosen for an efficient signal generation, required the use of suitable optics to generate three co-propagating beams travelling at the corners of a square before focalisation by a lens ($f = 1000$ mm). The two pump beams had the same energy, while the probe beam was four times weaker. The interaction region was a cylinder with a volume of 7.85 mm^3 with 1 cm of length along the beam propagation direction.

The FDFWM signal emerged from the interaction region, located at the centre of the 60 cm long optical cell, as if originating from the fourth corner of the square. The signal, after being spatially filtered, was detected by a photomultiplier tube connected to a Boxcar Averager (SRS245). The dye laser scan and data acquisition were simultaneously controlled by a PC (Epson 386DX). In the recorded spectrum each data point corresponded to the average of signals from 10 subsequent laser shots.

FeI atomic vapours was generated by raising up to 673 K the temperature of the cell filled with a mixture of 10 mbar of $Fe(CO)_5$ and 190 mbar of Ar. The cell was equipped with a Pt/Rh thermocouple to measure the gas temperature.

The effect of disregarding the atomic motion on DFWM line intensities has been considered for the present experimental parameters. The derivation of Eq. (3) does not include the washing-out effect of the induced grating due to the motion of the resonant species, which is more and more important as temperature increases. Here the angle θ under which the two pump beams were crossed was 0.74°, thus resulting in a fringe spacing equal to 23 μm. Since at 673 K the mean velocity of the FeI atom is 350 m/s, which corresponds to a mean free path of 5.25 μm during a 15 ns laser pulse, the assumption made in neglecting the atomic motion is justified.

4. Experimental results

Iron pentacarbonyl vapours exhibit a strong broad absorption band between 200 and 400 nm [19]. The thermal decomposition of $Fe(CO)_5$ was monitored in the temperature range 297–573 K by

measuring the transmission through the cell of a weak laser pulse (10 μJ energy) tuned at 302.2 nm on this broad band. The experimental data, shown in Fig. 2, indicate that at room temperature the laser radiation is completely absorbed by the $Fe(CO)_5$ vapours and that the transmission of the laser pulse increases with temperature due to the thermal decomposition of the $Fe(CO)_5$ molecule, which is completed around 523 K in good agreement with previous results [16].

The lineshape associated to the a^5D_2–$y^5D_2^0$ transition has been recorded at a temperature of 673 K with $I_P = 100$ μJ and $I_P = 200$ μJ. Synthetic lineshapes through the experimental curves have been evaluated according to [17], the results are shown in Fig. 3 for $I_P = 100$ μJ.

The calculated Rabi frequency in this experimental configuration is 0.034 cm^{-1}, with S laser beam diameter in the interaction region of 1.0 mm and $\mu_{ij} = 0.028$ D as determined by the relation

$$\mu_{if} = \frac{1}{g_i g_f}\sqrt{\frac{3\hbar e^2 f_{if}}{2m_e\omega_{if}}}, \tag{6}$$

where $f_{if} = 0.024$ and $\omega_{if} = 4.09$ eV/h are the oscillator strength and the frequency of the transition, respectively, and g the involved level degeneracy. The lifetime of the $y^5D_2^0$ level is 6.5 ns [2], which gives a value of 4.1×10^{-3} cm^{-1} for the

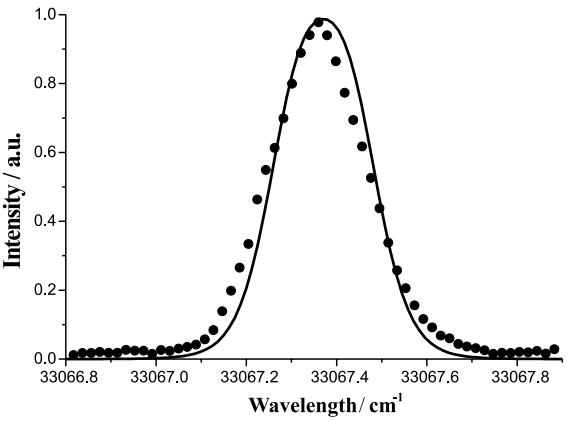

Fig. 3. Experimental lineshape (dots) of the a^5D_2–$y^5D_2^0$ transition in FeI at 673 K. Pump beam energy was 100 μJ. The continuous curve is a theoretical simulation with $S = 0.93$.

excited state population lifetime γ_{aa}. The closest agreement was achieved for $\gamma_{ab} = 0.3$ cm^{-1}, which corresponds to $S = 0.93$. In Fig. 4 the spectrum recorded at $I_P = 200$ μJ is reported together with the theoretical simulation performed with $S = 1.86$. The presence of a dip at the centre of the experimental FDFWM lineshape is clearly observable. The adopted model reproduces with good accuracy the lineshape, and the apparent discrepancies are ascribable to the multi-mode axial structure of the laser emission. In fact, due to

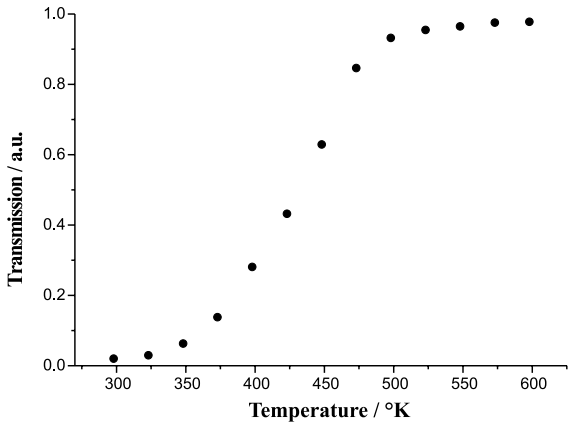

Fig. 2. Transmission of a laser pulse at 302.2 nm through a cell filled with 10 mbar of $Fe(CO)_5$ and heated up to 600 K. Transmission increases with temperature due to the thermal decomposition of $Fe(CO)_5$ absorbing the laser beam.

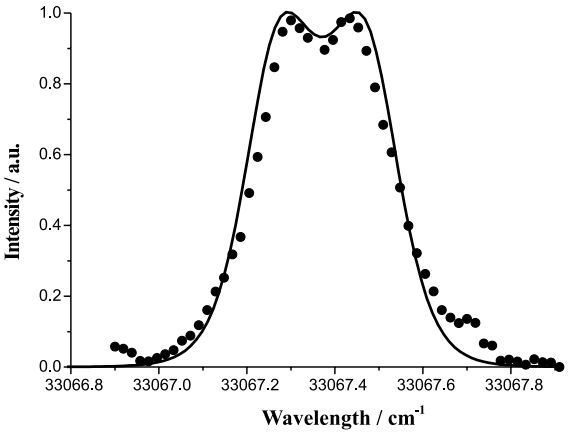

Fig. 4. Experimental lineshape (dots) of the a^5D_2–$y^5D_2^0$ transition in FeI at 673 K. Pump beam energy was 200 μJ. The continuous curve is the result of theoretical simulation with $S = 1.86$.

the non-homogeneous energy spatial distribution in the focal volume, regions which contribute to FDFWM signal with different degrees of saturation, may coexist. It is evident that saturation induces strong lineshape distortions in Fe DFWM spectrum, which completely hinder the application of this technique for quantitative measurements of physical parameters at high laser intensity.

Consequently, FeI FDFWM spectrum of the a^5D_j–$y^5D^0_j$ band was recorded at an excitation energy $I_P = 100$ μJ, below the saturation threshold. The normalised spectra recorded at 673 K and after cooling the dissociated gas mixture at 298 K are reported in Fig. 5. From lines assignment the a^5D_j–$y^5D^0_j$ ($j = 2, 3, 4$) transitions of FeI could be identified. An unassigned broad structure, not originating from any FeI transition, was also observed. The experimental evidence that its intensity drops to zero at room temperature suggests that it belongs to a hot band of some $Fe(CO)_{x=1,\ldots,4}$ molecular fragments.

The lines intensity ratios, in both spectra of Fig. 5, show divergences from the expected values in the approximation of optically thin medium and thermally distributed atomic population. As a matter of fact, at 298 K the population of the a^5D_4 level is ten times the one of the a^5D_3 level, thus the a^5D_4–$y^5D^0_4$ transition, appearing slightly weaker, should be nearly 100 times stronger than the a^5D_3–$y^5D^0_3$ line.

Deviations from the expected distribution are even more pronounced at 673 K, where the a^5D_2–$y^5D^0_2$ line becomes stronger than the a^5D_4–$y^5D^0_4$ fundamental transition.

The possible occurrence of spurious FeI DFWM signals due to $Fe(CO)_5$ photolysis [20–22] was analysed by repeating the experiment with 1 mbar of pure $Fe(CO)_5$ at room temperature. Since no DFWM signal generation was observed, it can be concluded that the amount of FeI produced by $Fe(CO)_5$ laser photolysis and in non-thermal distribution remained below the detection limit (∼10

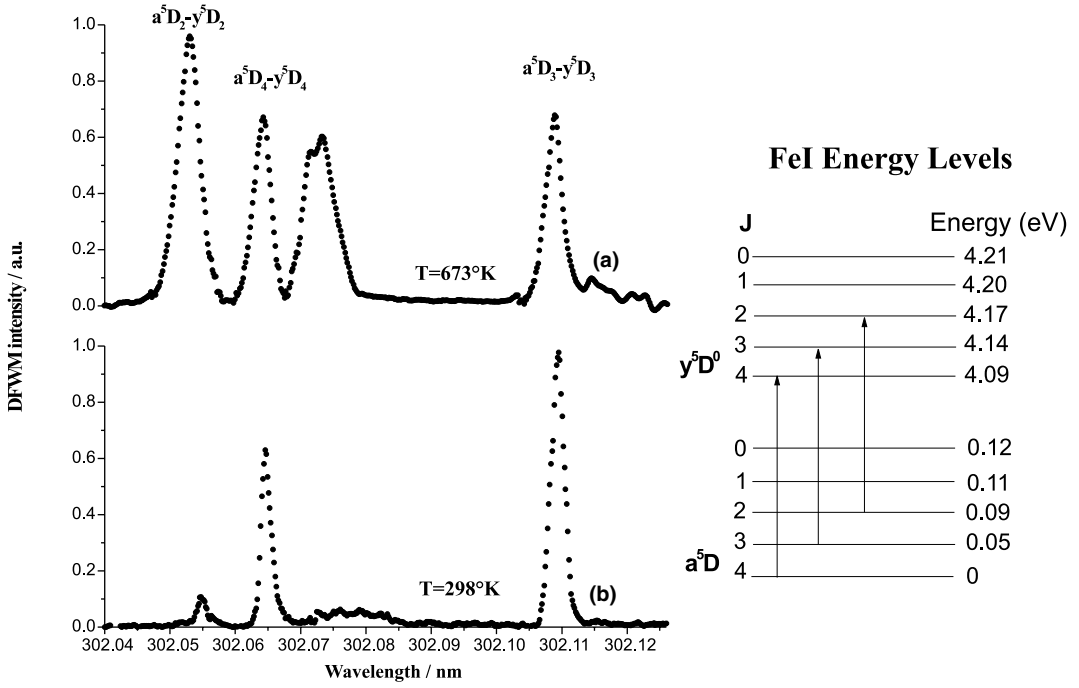

Fig. 5. Spectrum of the a^5D_j–$y^5D^0_{j'}$ system of FeI recorded at 673 K (a) and after having cooled the vapours at 298 K (b). Lines assignment allowed to identify the a^5D_j–$y^5D^0_j$ ($j = 2, 3, 4$) transitions of FeI. A scheme of the pertinent energy levels of FeI with the relevant transitions marked by arrows is shown on the right side.

ppm) of the experimental apparatus. This experimental finding suggests that the thermally produced FeI atoms populate the excited levels according to the Boltzmann law and that the anomalous line intensity ratio's can be ascribed only to the strong effect of pump beams depletion and signal re-absorption.

Accordingly, the FeI DFWM spectrum measured at room temperature was used to fit the parameters in Eq. (3). The obtained values $\alpha = 1$ and $\beta = 2.7$ were subsequently used to predict intensity ratio at 673 K. The results are compared in Table 1 with the results of calculations performed without ($\beta = 0$) and with ($\alpha = 1, \beta = 2.7$) absorption effects. The applied model provides a reasonable estimate of the experimental data (within 10% accuracy). Possible local temperature gradients inside the cell, likely to occur in the proximity of the optical windows, can be responsible for the observed differences.

The physical meaning of the β parameter deserves further attention. In our experimental setup the pump beams, with an intensity very close to the saturation value, show a linear attenuation different from both the weak probe and the signal beams, which obey an exponential absorption law. It follows that the exact factor, which should be used in Eq. (3) is:

$$(1 - \alpha N_i)^2 e^{-2\alpha N_i}. \tag{7}$$

It is impossible to estimate α with simple mathematical approaches, therefore the composite absorption effects have been replaced with the approximating factor of Eq. (3). This procedure greatly simplified the calculations despite the need of an additional parameter (β).

To quantify the degree of approximation, which the simplified treatment implies, for a given pair of α and β values, a function $G(x)$ can be defined as

$$G(x) = \left|(1 - 0.1x)^{2.7} - e^{-0.2x}(1 - 0.1x)^2\right|, \tag{8}$$

where x $(0 < x < 0.5)$ is the fraction of atoms in an excited level normalised to the ground state population. This function represents how much the approximated correction factor disagrees from the exact value. In the present case we have $G(x) \sim 0.1x$. Since in our experimental conditions we observed at most $x \approx 0.33$, $G(x)$ can only span between 0 and 0.033, thus confirming the validity of the proposed simplified approach.

5. Discussion and conclusions

The spectrum of the a^5D_j–$y^5D^0_{j'}$ system of FeI recorded with a non-linear spectroscopic technique (DFWM) based on scattering from laser induced gratings in a gaseous medium is reported for the first time. FeI atomic vapours were produced by heating up to 673 K iron pentacarbonyl vapours. The ratio between the length of the region in which signal is generated and the length of the optical cell filled with FeI vapours being nearly equal to 1.6×10^{-2}, strong absorption effects on DFWM signal were observed in spectra at 673 K and room temperature. This observation is consistent with the analysis of Ewart [23], who demonstrated that Na vapours, in the same pressure range as used in our experiment, becomes optically thick over a length of about 5 cm. With the purpose to demonstrate that absorption effects can strongly alter the expected line intensities, a simple model was

Table 1
Experimental and calculated lines intensity ratio of a^5D_j–$y^5D^0_j$ DFWM spectrum of FeI (at 298 and 673 K)

Ratio designation[a]	Measured ($T = 298$ K)	Calculated[b] ($T = 298$ K)	Calculated with correction[c] ($T = 298$ K)	Measured ($T = 673$ K)	Calculated[b] ($T = 673$ K)	Calculated with correction[c] ($T = 673$ K)
I_{22}/I_{44}	4×10^{-2}	7×10^{-5}	3.3×10^{-2}	1.54	4×10^{-3}	1.68
I_{33}/I_{44}	1.6	4×10^{-3}	1.54	1.14	4×10^{-2}	1.33
I_{22}/I_{33}	2.5×10^{-2}	1.7×10^{-2}	2.3×10^{-2}	1.39	0.1	1.27

[a] In this notation the intensity of the a^5D_j–$y^5D^0_j$ line is designed as I_{jj}.
[b] Value calculated assuming thermal distribution and no absorption effects (optically thin medium).
[c] Value calculated with Eq. (3), $\alpha = 0.1$ and $\beta = 2.7$ (optically thick medium).

proposed to reproduce the experimental findings. This model gives reasonable agreement with data (10% accuracy), without the need of introducing awkward numerical calculations.

The a^5D_2–$y^5D_2^0$ transition was chosen to monitor the saturation effect on FeI DFWM lineshape at 673 K since among the recorded lines it is less affected by pump beams depletion. The evidence of line-splitting due to saturation indicates that atomic vapours are targets which can significantly contribute to shed light on the physical nature of the saturation line-splitting in DFWM. It is worthwhile to mention that in our previous experiment dealing with saturated DFWM on NO_2 molecule no evidence for such a dip was observed [24]. The induced dipole moment in FeI ($\sim 3 \times 10^{-2}$ D) is considerably lower than in NO_2 (~ 0.4 D), this difference is rather general in comparing atoms with molecules and in our opinion may help towards a deeper comprehension of their different saturation behaviour. Finally it has to be pointed out that we choose Ar as buffer gas because it has a lower quenching cross-section for FeI with respect to N_2 [25], thus allowing to minimise the contribution to signal due to thermal grating formation. Nevertheless, by suitably delaying the probe beam, significant information on the collisional energy redistribution processes in FeI, as a function of different buffer gases, can be obtained from DFWM signals.

Acknowledgements

We would like to thank S. Pignataro, B. Attal Tretout and G. Gatti for helpful discussions. The contribution of M. Giorgi at the early stage of the work is gratefully acknowledged.

References

[1] J. Sugar, C. Corliss, J. Phys. Chem. Ref. Data 14 (Suppl. 2) (1985).
[2] T.R. O'Brian, M.E. Wickliffe, J.E. Lawler, W. Whaling, J.W. Brault, J.Opt. Soc. Am. B 8 (1991) 1185.
[3] F. Orsitto, M. Borra, F. Coppotelli, G. Gatti, Rev. Sci. Instrum. 66 (1995) 597.
[4] P. Ewart, S.V. O'Leary, Opt. Lett. 11 (1986) 279.
[5] T. Dreier, D.J. Rakestraw, Appl. Phys. B 50 (1990) 479.
[6] S. Williams, R.N. Zare, L.A. Rahn, J. Chem. Phys. 101 (1994) 1093.
[7] P. Ljungberg, O. Axner, Appl. Phys. B 63 (1996) 69.
[8] D.H. Bloom, P.F. Liao, N.P. Economou, Opt. Lett. 2 (1978) 58.
[9] N. Tan-no, T. Hashimiya, H. Inaba, IEEE J. Quant. Electron. QE 16 (1980) 147.
[10] G.P. Agrawal, A. Van Lerberghe, P. Aubourg, J.L. Boulnois, Opt. Lett. 7 (1982) 540.
[11] G. Grynberg, M. Pinard, P. Verkerk, Opt. Commun. 50 (1984) 261.
[12] G. Grynberg, M. Pinard, P. Verkerk, J. Physique 47 (1986) 617.
[13] Z. Karny, R. Naaman, R.N. Zhare, Chem. Phys. Lett. 59 (1978) 33.
[14] D.W. Trainor, S.A. Mani, J. Chem. Phys. 68 (1978) 5481.
[15] J.T. Yardley, B. Gitlin, G. Nathanson, A.M. Rosan, J. Chem. Phys. 74 (1981) 370.
[16] S. Pignataro, F.P. Lossing, J. Organomet. Chem. 11 (1968) 571.
[17] B. Attal Tretout, H. Bervas, J.P. Taran, S. Le Boiteux, P. Kelley, T.K. Gustafson, J. Phys. B 30 (1997) 497.
[18] W.P. Brown, J. Opt. Soc. Am. 73 (1983) 635.
[19] M. Kotzian, N. Rösch, H. Schröder, M.C. Zerner, J. Am. Chem. Soc. 111 (1989) 7687.
[20] S.A. Mitchell, P.A. Hackett, J. Chem. Phys. 93 (1990) 7813.
[21] K. Lee, J.S. Goo, J.K. Ku, Chem. Phys. Lett. 244 (1995) 213.
[22] L. Bānares, T. Baumert, M. Bergt, B. Kiefer, G. Gerber, J. Chem. Phys. 108 (1998) 5799.
[23] P. Ewart, S.V. O'Leary, J. Phys. B 17 (1984) 4595.
[24] R. Fantoni, L. De Dominicis, M. Giorgi, R.B. Williams, Chem. Phys. Lett. 259 (1996) 342.
[25] S.A. Mitchell, P.A. Hackett, J. Chem. Phys. 93 (1990) 7813.